Available online at www.sciencedirect.com

SciVerse ScienceDirect

Ceramics International 39 (2013) 691–699

CERAMICS INTERNATIONAL

www.elsevier.com/locate/ceramint

Effect of high energy milling process on microstructure and piezoelectric/dielectric properties of $K_{0.475}Na_{0.475}Li_{0.05}NbO_3$ solid solution

Soon-Chul Ur, Iqbal Mahmud, Man-Soon Yoon*

[a]*Department of Materials Science and Engineering/RIC-ReSEM, Chungju National University, 72 Daehakgno, Chnugju, Chungbuk 380-702, Republic of Korea*

Received 10 February 2012; received in revised form 18 June 2012; accepted 26 June 2012
Available online 30 June 2012

Abstract

$K_{0.475}Na_{0.475}Li_{0.05}NbO_3$ (abbreviated as NKLN) ceramic of near the morphotropic phase boundary (MPB) composition was synthesized by two different processes. The first one is the high energy milling [sometimes abbreviated as HEM hereafter] process, which involves mixing the starting materials and milling the calcined powder using a high energy nano-mill, in order to obtain nano-sized particles. The second one is a conventional mixed oxide method. The HEM process of the starting materials lowered the calcination temperature to the extent of 200 °C as compared with conventionally fabricated NKLN. The particle size of the powder, exposed to the HEM process, reduced to 40 nm, whereas the conventionally ball-milled powder had a larger size of 420 nm after the mixing process. Furthermore, the HEM process improved the reaction activity and homogeneity of the materials used throughout the process, accompanying the enhancement of the sintering density, grain uniformity, and the decrease of grain size. In order to investigate the effects of the HEM process on the electric properties of NKLN ceramics, the dielectric and piezoelectric properties of sintered specimens fabricated by two different processes were evaluated. It was found that the properties of the nano-sized NKLN ceramic near the MPB composition were increased by the modified method, showing the maximum values of $d_{33}=179$ pC/N, $k_p=34\%$ and $K_{33}^T=440$ compared with 132 pC/N, 29%, and 400, respectively in the conventional process. Further evidence for the grain size effect was investigated by the polarization–electric field curve at room temperature. The remnant polarization for the nano-sized NKLN specimen had a higher value of 24.3 μC/cm^2 compared with that of 13.7 μC/cm^2 for conventional NKLN, whereas the coercive field had a similar value. The modified mixing and milling method was considered to be a new and promising process for lead-free piezoelectric ceramics owing to their excellent piezoelectric/dielectric properties.

Keywords: Milling; Grain size; X-ray methods; Piezoelectric properties

1. Introduction

Lead oxide based ferroelectric materials such as lead zirconate titanate (PZT) are the most widely used ceramics for leading edge technology applications such as actuators, sensors and transducers. The environmental and health hazards of lead are well-known and recycling and disposal of devices containing lead-based piezoelectric materials are of great concern.

Thus, it is necessary to develop lead-free piezoelectric materials. However, until now, no effective alternatives to PZT have been found. Since the end of the 1990s, researchers have paid much attention to lead free piezoelectrics, especially to $[Bi_{0.5}Na_{0.5}]TiO_3$ (BNT) and $[Na_{0.5}K_{0.5}]NbO_3\cdot$(NKN). In particular, after the development of textured NKN-based ceramics [1], researches on lead free piezoelectric ceramics have been progressively performed, claiming that new piezoelectric ceramics should be lead free within the next few decades. In particular, most of the recent work has focused on the NKN perovskite system because of its high Curie temperature and piezoelectric constant. However, major drawbacks

*Corresponding author. Tel.: +82 43 841 5804; fax: +82 43 841 5805.
E-mail address: msyoon@cjnu.ac.kr (M.-S. Yoon).

0272-8842/$36.00
http://dx.doi.org/10.1016/j.ceramint.2012.06.080

regarding NKN ceramics still exist, such as the need for special handling of starting powders in synthesis, the property sensitivity to nonstoichiometry and the inherent difficulties in densification [2–5]. In order to address these problems, various consolidation techniques have been considered such as hot pressing and the spark plasma sintering process [2,6,7]. Synthesis by high-energy ball milling is known to reduce the calcination temperature, alter the entire calcination step and further reduce the loss of alkali metal oxides [8,9]. Different types of dopants or additives are preferentially added in NKN to form new ceramic solutions with improved piezoelectric properties. These include NKN–$LiNbO_3$–$AgSbO_3$ [10], NKN–$LiNbO_3$ [11], NKN–$LiNbO_3$–$CaTiO_3$ [12], NKN–$LiNbO_3$–$AgNbO_3$ [13], NKN–$LiSbO_3$ [14] and so forth. Although these methods could yield higher densities and better properties, extra care for the investigation and optimization of sintering parameters must be taken into account in order to obtain reproducible and high quality materials. In this work, a new fabrication technique was considered to overcome some of the problems discussed above, and to provide improved piezoelectric properties in the NKN system.

The main purpose of this present study is to control the size and morphology of the powder mixture in order to increase the reaction activity using a high energy nano mill. In addition, we also plan to demonstrate the effect of nano-sized NKLN particles on the microstructure and the piezoelectric/dielectric properties.

2. Experimental procedure

Perovskite $Na_{0.475}K_{0.475}Li_{0.05}NbO_3$ [abbreviated as NKLN] was fabricated by the two processes previously mentioned. The first process is designated as process I, which is conducted by the high-energy milling process of mixed and calcined powder [sometimes abbreviated as nano-sized NKLN] and the other is designated as process II, for which the process of mixing and milling is performed by the conventional ball mill process [sometimes abbreviated as conventional NKLN]. The detailed fabrication process was shown in Fig. 1. Before synthesizing the NKLN, all of raw materials were heat treated at 250 °C for 5 h to remove the absorbed water molecules and kept in a vacuum chamber. For process I, raw materials of the analytical-reagent (AR) grade K_2CO_3 (99%, High Purity Chem. Co.), Na_2CO_3 (99%, High Purity Chem. Co.), Li_2CO_3 (99%, High Purity Chem. Co.) and Nb_2O_5 (99.8%, Sakai Chem. Co.) were weighed to their stoichiometry and mixed in a high-energy mill (NETZSCH, MINICER, D-95100) to effectively eliminate the problems associated with size differences and to obtain nano-sized particles. After drying the powder mixture, calcination was carried out at 600 °C for 4 h. The calcination temperature was chosen based on the

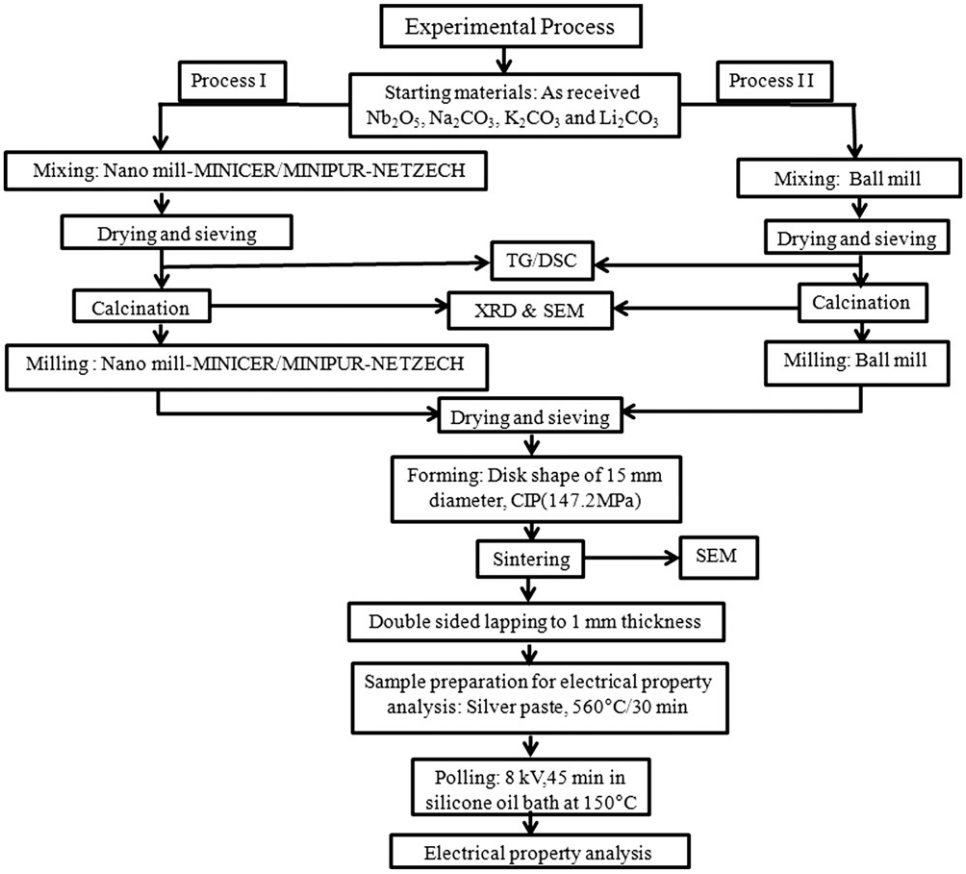

Fig. 1. Processing block diagram for NKLN preparation (process I: high energy milled NKLN and process II: conventional NKLN).

TG/DSC analysis. An additional milling step with HEM was then performed in order to reduce the particle size of the calcined powder. The mixing and milling processes were conducted in ethanol with the mixed zirconia beads of 0.2 and 0.1 mm diameter for 1 h with a rotor speed of 3500 rpm using HEM.

To compare the properties of high-energy milled NKLN powder with those of conventionally prepared NKLN powder, the NKLN powder having the same composition as in process I was synthesized by using a conventional ball-mill process. Raw materials of analytical-reagent (AR) grade were weighed and ball-milled in a ZrO_2 mediaum ethanol for 24 h. The dried powder was then calcined at 800 °C for 4 h. An additional ball-milling step of the calcined powder was added to ensure the fine particle size before sintering. The dried powders prepared from the two different processes were first pressed as a disk to a diameter of 15 mm and then cold-isostatically pressed again under 147.2 MPa without a binder. According to the preliminary study, at which the sintering time of 3 h for process I had given rise to maximum properties at various sintering temperatures, the sintering time of all samples used in the study was kept at 3 h. The CIPed samples were sintered at various temperatures for 3 h. To limit the loss of alkali metal ions having a high vapor pressure, a similar way to the double crucible method [15] was adopted as shown in Fig. 2. The inner Al_2O_3 crucible includes the pressed samples lying on the NKLN substrate having the same composition as the samples. The external Al_2O_3 crucible was filled with the mixed NKLN powder and the inner Al_2O_3 crucible was covered with the Al_2O_3 lid and buried in the external Al_2O_3 crucible. After burying the inner crucible, the external Al_2O_3 crucible was also covered with the Al_2O_3 lid. The sintered samples were then polished to obtain a parallel surface up to a thickness of 1 mm. The two kinds of the powders fabricated from both processes I and II were characterized by an X-ray diffractometer (XRD, Rigaku D/Max-2500H, Japan) with Cu Kα radiations after calcination and sintering. Powder morphologies and microstructures for all of the ceramic samples were investigated using a scanning electron microscope (Hitachi S-2400 and FEI Company Quanta-400). In order to measure the electrical properties, silver paste was coated to form electrodes on both sides of the sample, and then subsequently fired at 560 °C for 30 min. For investigating the proper poling condition, each specimen was first poled in stirred silicon oil at 150 °C, by applying a dc electric field of 4–8 kV/mm for 45 min and subsequently aged at 120 °C for 3 h. The dielectric and the piezoelectric properties of the aged samples were then measured and evaluated. Based on the results, the optimum poling voltage was decided to be 8.0 kV/mm, considering the fact that standard deviation of the electric properties could exist in the measured samples, we prepared and measured 5 specimens on each of the samples. The piezoelectric coefficient was determined using a d_{33} meter (IACAS; Model ZJ-6B), and the electromechanical, and dielectric properties were calculated by a resonance/anti-resonance measurement method [16] using an impedance/gain phase analyzer (HP- 4194A). Temperature dependence of the dielectric constant and the dissipation factor over a range from −40 to 500 °C was measured using an automated system at various frequencies at 1 kHz, whereby HP-4194A and a temperature-control box (−40–150 °C: Delta 9023 chamber, 150–500 °C: Lindberg tube furnace) were controlled by a desk-top computer system. The temperature was measured using a Keithley 740 thermometer via a *K*-type thermocouple mounted on the samples. The behavior of the polarization-electric field was determined using a Precision LC system (Radiant Technology Model: 610E).

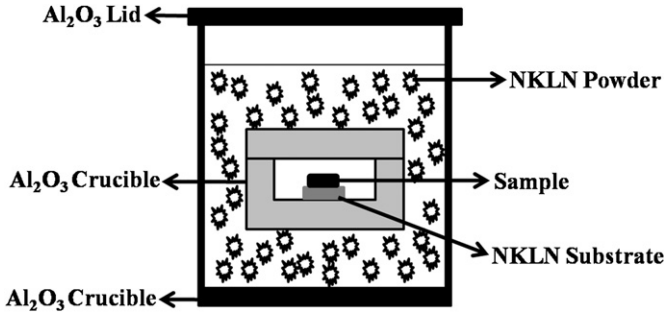

Fig. 2. Schematic illustration of double enclosed alumina crucible method for the sintering of $K_{0.475}Na_{0.475}Li_{0.05}NbO_3$ ceramics.

3. Results and discussions

3.1. Effects of nano-sized particles on the reaction temperature and powder morphology of NKNL

In order to investigate the effect of nano-sized particle of the starting powders on the reaction temperature and powder morphology of NKLN, the starting powders were milled using the high-energy mill. Fig. 3 shows the SEM micrographs of as-received powders and Fig. 4(a), and (b) exhibits powders fabricated by processes I and II, respectively. When compared to each other, it can be seen that process I results in reduced particle size along with homogeneity, while process II shows relatively larger particle size (~420 nm) with irregular shape. The average particle size of the NKLN synthesized by process I is ~40 nm with the spherical shape, whereas that by process II has a broader particle size distribution. It indicates that the high-energy milling process results in reduced particle size and enhances reaction activities, leading to a decrease in calcination temperature. In contrast, the mixed powders fabricated by the ball milling process showed an irregular shape with broad particle size distribution and coarse particles. Therefore, it can be speculated that the conventional mixing process induces an increase in calcination temperature.

Morphologies of calcined powders synthesized by processes I and II are presented in Fig. 5(a) and (b), respectively. It can be seen that the high-energy milled

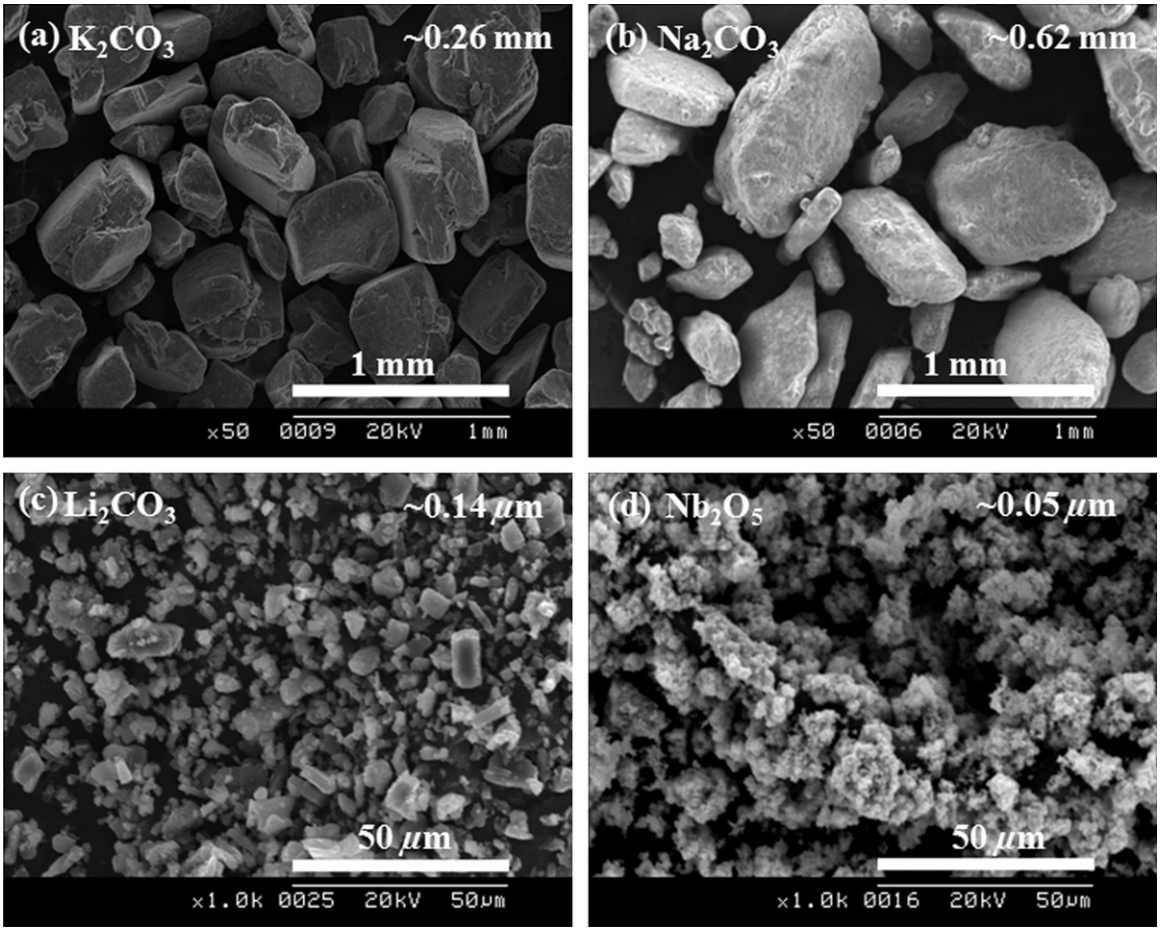

Fig. 3. SEM micrographs of the as-received starting materials used in the synthesis of NKLN.

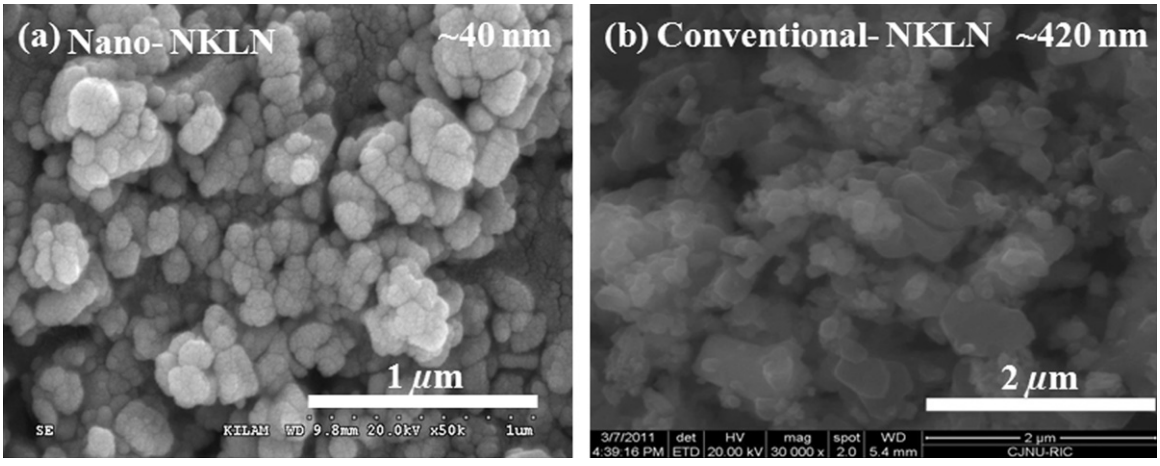

Fig. 4. SEM micrographs of high energy milled NKLN and conventional NKLN.

NKLN has a fine and sphere shaped particle morphology with homogeneity, while the conventional process shows relatively larger particle size with irregular shape. Fig.5(c) shows the X-ray diffraction patterns of the calcined NKLN samples fabricated through processes I and II. All of them are fully stabilized to the perovskite structure without the second and/or pyrochlore phases. Especially, despite a low calcination temperature, the second and/or pyrochlore phases did not exist in the nano-sized NKLN. As shown in Fig. 5(a), and (b), the nano-sized NKLN has an average particle size of ~100 nm, with near spherical and narrow size distribution. In contrast, the conventional one shows an irregular shape with broad particle size distribution having an average particle size of ~350 nm. In

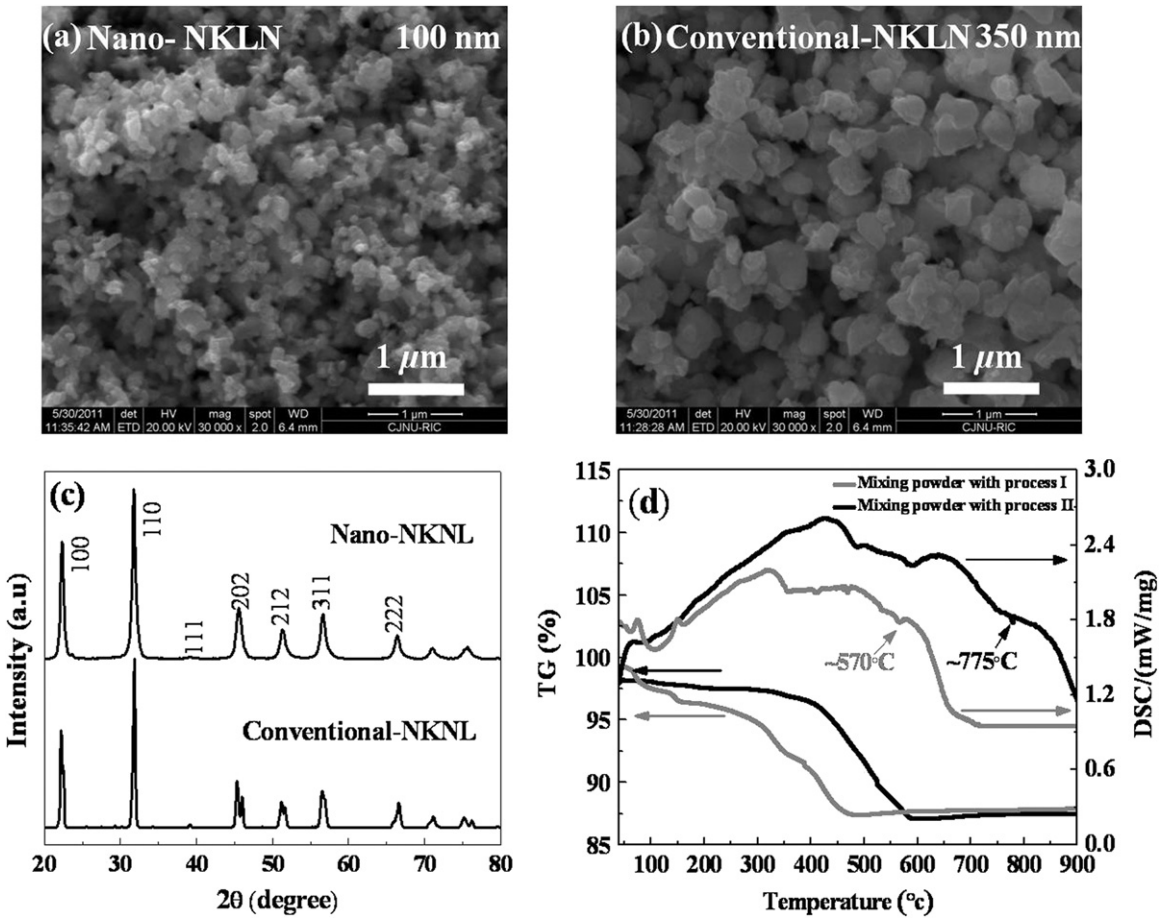

Fig. 5. The powder morphology and X-ray diffraction patterns of calcined NKLN: (a) SEM micrograph of nano NKLN, (b) SEM micrograph of conventional NKLN, (c) X-ray diffraction patterns, and (d) TG–DSC of high energy milled and conventional NKLN.

addition to this, it can be noted that the peak splitting appeared at (220) and (002) orthorhombic reflection for the calcined powder fabricated by the conventional process, whereas this peak splitting disappeared at $2\theta \sim 45^{o}$ for the nano-sized NKLN sample, indicating the cubic phase as shown in Fig. 5(c). This result can be interpreted as a size effect [17,18]. Uchino et al. [17] reported in the $BaTiO_3$ system that the decrease of the tetragonal phase in fine-grained $BaTiO_3$ was due to surface tension. According to them, this surface tension is sufficiently high to decrease the tetragonality in the fine particle sized $BaTiO_3$. A more detailed report on the size effect was reported by Begg et al. [18]. They reported that hydrothermal $BaTiO_3$ powder with a particle size larger than 270 nm was a completely tetragonal phase, while hydrothermal $BaTiO_3$ powder for a particle size less than 190 nm was a fully cubic phase. Since the high-energy milling process lowers the reaction temperature and then reduces the particle size to 100 nm as shown in Fig. 5(a), it is highly probable that the NKLN powder fabricated by process I has a relatively lower anisotropic (for example cubic phase) compared to the conventional NKLN.

To observe the effect of the high-energy milling process on the calcination temperature, the thermo-gravimetric/differential scanning calorimetry (TG/DSC analysis) was performed and the results were presented in Fig. 5(d). From the TG/DSC results, the high-energy milling process of the starting materials seems to be effective in decreasing the reaction temperature, showing a temperature difference of $\sim$200 °C as shown in Fig. 5(d). In addition to these results, weight loss due to the removal of carbonate was advanced in the high-energy milled NKLN powder, suggesting the increase in surface area and activity. Based on the analysis above, the mixtures prepared by processes I and II, were calcined at 600 °C and 800 °C, respectively. This in turn suggests that the fine starting material of NKLN enhances the solid–solid reaction and decreases the reaction temperature due to their high activity.

3.2. Effects of the nano-sized NKLN powder on the microstructure and the piezoelectric/dielectric properties

According to the previous results, the high-energy milling process lowered the calcination temperature of NKLN, suggesting a change of the microstructure and the piezoelectric/dielectric properties. The microstructures of the sintered NKLN samples were observed by SEM. The micrographs of the nano-sized NKLN samples for

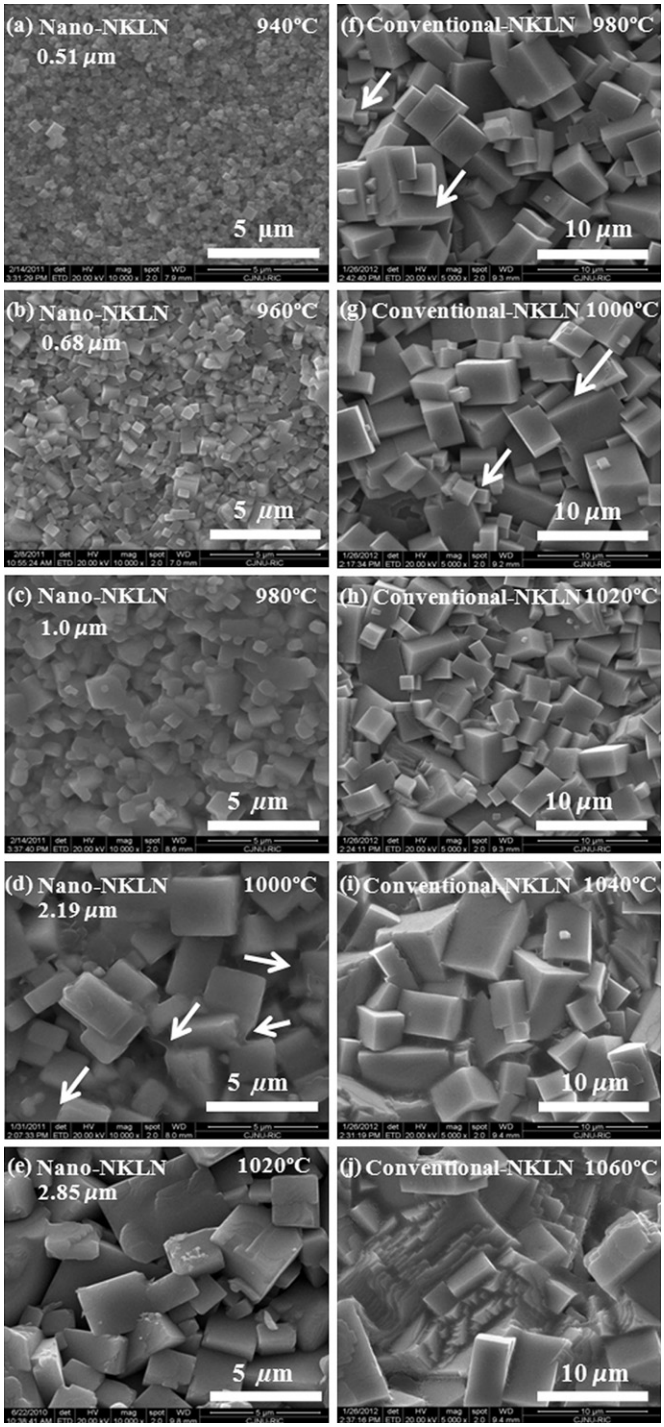

Fig. 6. SEM micrograph of nano-sized NKLN sintered at (a) 940 °C, (b) 960 °C, (c) 980 °C, (d) 1000 °C, and (e) 1020 °C for 3 h and conventional NKLN sintered at (f) 980 °C (g) 1000 °C (h) 1020 °C (i) 1040 °C , and (j) 1060 °C for 3 h.

various sintering temperatures are shown in Fig. 6(a)–(e), compared with those of the conventional NKLN sample of Fig. 6(f)–(j). As can be seen, the grain shape of all samples was cubic. In case of nano-sized NKLN, average grain size gradually increased when the sintering temperature was increased. The increase for the average grain size slightly depends on the sintering temperature below 980 °C with a clear grain boundary and a dense microstructure, while it abruptly increased above 1000 °C, accompanying the disappearance of the grain boundary clarity. This grain coarsening could have possibly occurred due to the liquid phase formation, which was designated by the arrow. A liquid phase, which may be formed in the grain boundary of ceramics when increasing the sintering temperature, results in the rapid increase of grain size [19,20]. A detailed analysis will be reported later. Fig. 6(f)–(j) shows the SEM morphologies of conventional NKLN samples as a function of sintering temperature; cubic-shaped grains without a clear grain boundary can be seen from all the samples. As shown in Fig. 6(f) and (g), there is a bimodal distribution of grain size for the samples sintered at 980 °C and 1000 °C. There are two kinds of grains. One is the smaller grain of ~1 μm and the other is the relatively larger one of ~4 μm, indicated by the arrows. As the sintering temperature increased to 1020 °C, the size difference was reduced with the grain growth of the small grains, while the size of larger grains was maintained as shown in Fig. 6(h).

Through further increase of the sintering temperature, the size difference virtually disappeared at 1040 °C by increase in the size of both small and large grains, as grain size abruptly increased at 1060 °C. This behavior looks similar to that of the nano-sized NKLN specimen. Therefore, it can also be predicted that a liquid phase appears at 1040 °C [19,20].

Furthermore, since the microstructure is directly associated with the sintering density, the variation densities of all samples as a function of sintering temperature are plotted in Fig. 7. As a result, the nano-sized specimen sintered at 980 °C shows a maximum value for the sintering density of 4.5 g/cm^3 compared to 4.28 g/cm^3 of the conventional NKLN sample sintered at 1020 °C, which then sharply decreased to 4.25 g/cm^3 and 3.83 g/cm^3, respectively, as the sintering temperature increased. Therefore, the observed clarity of grain boundary seems to be closely related with the increase of sintering density.

To observe the effects of grain size on the piezoelectric and dielectric properties, the variation of these properties at various sintering temperatures are plotted in Fig. 8(a)

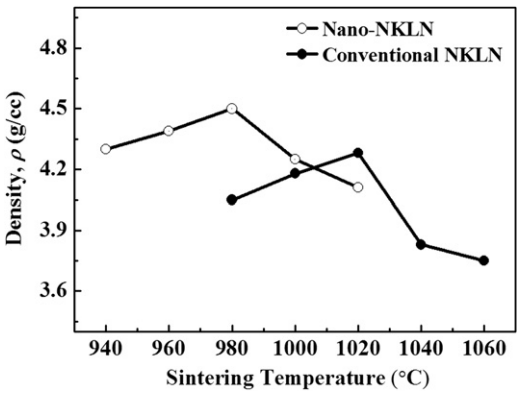

Fig. 7. Change in sintered density for nano and conventional NKLN ceramics as a function of sintering temperature.

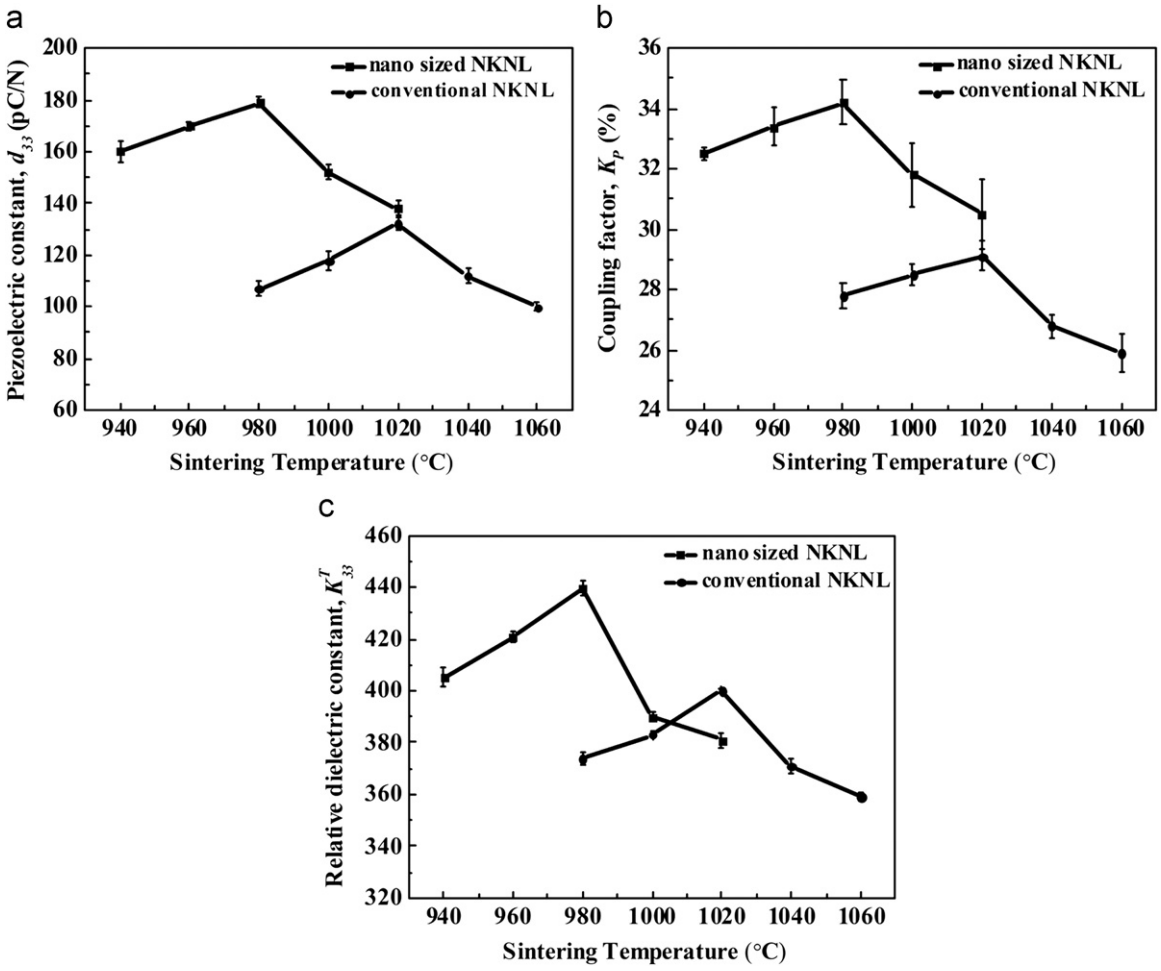

Fig. 8. Variation of piezoelectric and dielectric properties as a function of sintering temperature in nano-sized NKLN and conventional NKLN: (a) piezoelectric constant (d_{33}), (b) planar electromechanical coupling factor (k_p), and (c) relative dielectric permittivity (K_{33}^T).

and(c). The electrical properties of NKLN samples synthesized by processes I and II were evaluated as a function of sintering temperature.

Comparing the results of piezoelectric properties for both processes, the modified process I significantly improved the piezoelectric properties of NKLN ceramics. As shown in Fig. 8 (a)–(b), the nano-sized NKLN sample sintered at 980 °C shows the maximum value of the piezoelectric coefficient (d_{33}) of 179 pC/N and the planar electromechanical coupling factor (k_p) of 34% and then decreased rapidly above 980 °C, where the clarity of grain boundary diminished. For the NKLN specimen fabricated by the conventional process, the samples sintered at 1020 °C showed the highest piezoelectric coefficient (d_{33}) and the planar electromechanical coupling factor (k_p) of 132 pC/N and 29%, respectively, which then decreased rapidly above 1020 °C.

Furthermore, it can be seen that process I lowers the optimal sintering temperature by 40 °C. It is worth noting that the changes in the piezoelectric properties are fairly small as long as the clarity of the grain boundary is maintained, but after this the d_{33} and k_p values steeply decreased.

The relative dielectric constants (K_{33}^T) of the two series were measured at a frequency of 1 kHz, and Fig. 8(c) shows the change in K_{33}^T as a function of the sintering temperature. For the nano-sized NKLN specimens, the highest dielectric constant (K_{33}^T) of 440 was obtained at 980 °C as shown in Fig. 8(c), while conventional NKLN specimens showed the maximum value of 400 for K_{33}^T at 1020 °C and then decreased to 390 and 380, respectively. The change in the dielectric constant was similar to that in density as a function of the sintering temperature as shown in Fig. 7.

Despite the increasing grain size, the dielectric constants for both samples decrease above the critical sintering temperature indicating the maximum density. In order to explain this phenomenon, SEM morphologies of the high magnification were observed for both samples. Fig. 9 shows the SEM morphology of the nano-sized NKLN specimen sintered at 1000 °C (Fig. 9(a)), compared to that of the conventional NKLN specimen sintered at 1040 °C (Fig. 9(b)).

As shown in Fig. 9, some liquid phases caused by the alkali metal ions, which are designated by the arrow, are

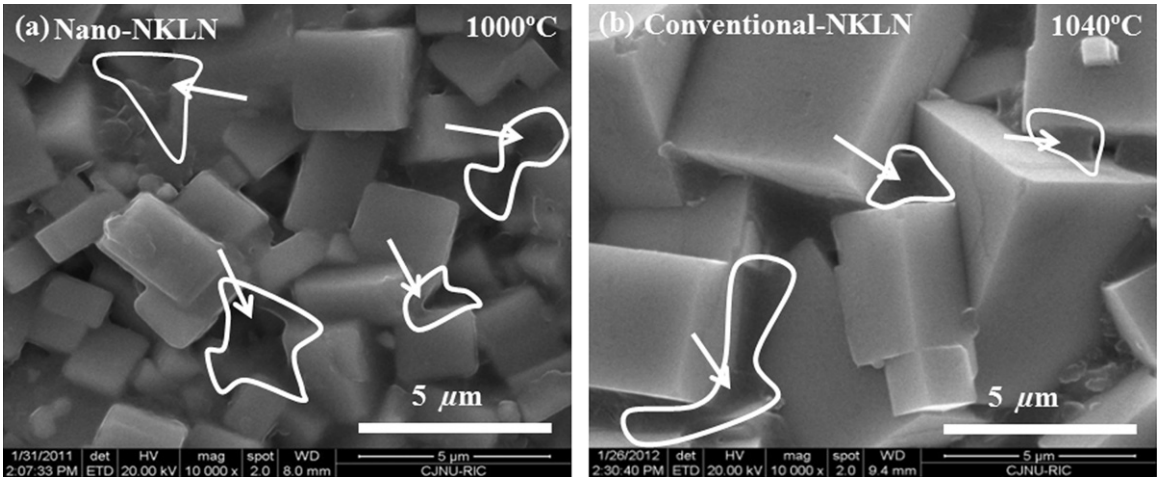

Fig. 9. SEM micrograph of high energy milled NKLN sintered at (a) 1000 °C and conventional NKLN sintered at and. (b) 1040 °C.

observed. In the case regarding the nano-sized NKLN specimen, the liquid phase appears at 1000 °C, which is 40 °C lower than that of the conventional NKLN. Since the high energy milling process reduced the particle size of calcined powder to nano scale resulting in the increase of surface energy, the particles exposed to high energy milling could melt even at 1000 °C as shown in Fig. 9(a). Therefore, it can be interpreted that the appearance of the liquid phase seems to play an important role in the decrease of the relative dielectric constant.

Further evidence for the grain size effect was obtained by examining the polarization–electric field (P–E) curve at room temperature as shown in Fig. 10. Since the piezoelectric/dielectric properties are directly associated with a behavior of the P–E hysteresis curves, both samples sintered at the critical temperature showing the maximum density are plotted in Fig. 7. The values of remnant polarization (P_r) and the coercive field (E_c) were determined from the measured loops. From the data of hysteresis loops, the remnant polarization P_r for the nano-sized NKLN specimen has a higher value of 24.3 μC/cm^2 compared with that of 13.7 μC/cm^2 for conventional NKLN, whereas the coercive field (E_c) has a similar value. These results were in agreement with the previous analysis of the piezoelectric/dielectric properties. Therefore, the increase of the piezoelectric and dielectric properties was to be closely related with the increase of P_r. These results indicate that homogenously mixed and milled nano-powders enhance the uniformity of the solid–solid reaction accompanying the increase of piezoelectric and dielectric properties.

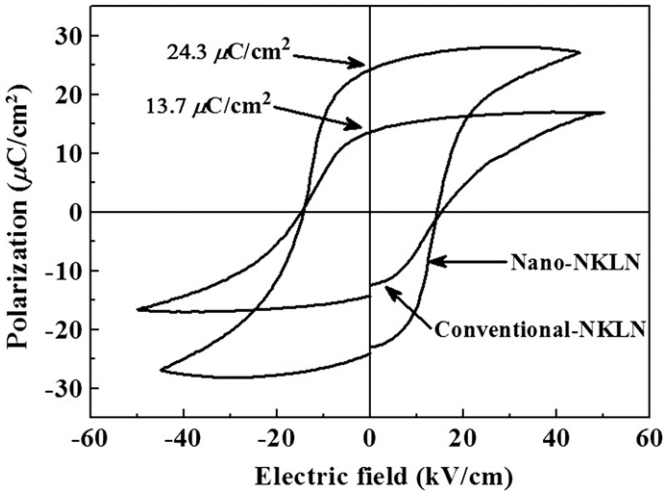

Fig. 10. The P–E curves for high energy milled NKLN and conventional NKLN at 25 °C.

4. Conclusion

The effects of the manufacturing process on the reaction temperature, microstructure and dielectric/piezoelectric properties have been analyzed systematically for NKLN ceramics of near MPB composition. In addition, the effects of nano-sized starting powder on the reaction temperature and the crystal structure have been examined. Our study revealed that the nano-milling process effectively lowered the reaction temperature for NKLN during calcination and sintering. A fully stabilized perovskite phase was observed in spite of the much lower reaction temperature for nano-sized NKLN. Besides, the peak of the calcined powder, fabricated by the high energy milling process, demonstrated a cubic phase, whereas the conventional one indicated the orthorhombic phase caused by the size effect. Through microstructure observations, significant improvement of grain morphology, sintered density and piezoelectric/dielectric properties were also enhanced in nano-sized NKLN compared to the conventional one. The variation of the piezoelectric and dielectric properties for the nano-sized NKLN could be interpreted on the basis of density. The highest value of d_{33} and k_p were found for the nano-sized NKLN sintered at 980 °C, which has been interpreted as the density due to the clarity of the grain

boundary. *P–E* hysteresis results also supported the fact that the increase of electric properties was closely related with the high energy milling process.

Acknowledgments

This research was supported by the Regional Innovation Center (RIC) Program, which was conducted by the Ministry of Knowledge Economy of the Korean Government.

References

[1] Y. Saito, H. Takao, T. Tani, T. Nonoyama, K. Takatori, T. Homma, T. Nagaya, M. Nakamura, Lead-free piezoceramics, Nature 432 (2004) 84–87.

[2] J. Rodel, W. Jo, K.T.P. Seifert, E-M. Anton, T. Granzow, Perspective on the development of lead-free piezoceramics, Journal of the American Ceramic Society 92 (6) (2009) 1153–1177.

[3] T.A. Skidmore, S.J. Milne, Phase development during mixed-oxide processing of a $[Na_{0.5}K_{0.5}NbO_3]_{1-x}$–$[LiTaO_3]_x$ powder, Journal of Materials Research 22 (8) (2007) 2265–2272.

[4] Y. Wang, D. Damjanovic, N. Klein, E. Hollenstein, N. Setter, Compositional inhomogeneity in Li- and Ta-modified (K, N_a)NbO_3 ceramics, Journal of the American Ceramic Society 90 (11) (2007) 3485–3489.

[5] Y. Wang, D. Damjanovic, N. Klein, N. Setter, High-temperature instability of Li and Ta modified (K,Na)NbO_3 piezoceramics, Journal of the American Ceramic Society 91 (6) (2008) 1962–1970.

[6] G.H. Haerting, Properties of hot-pressed ferroelectric alkali niobate ceramics, Journal of the American Ceramic Society 50 (6) (1967) 329–330.

[7] J.F. Li, K. Wang, B.P. Zhang, L.M. Zhang, Ferroelectric and piezoelectric properties of fine-grained $Na_{0.5}K_{0.5}NbO_3$ lead-free piezoelectric ceramics prepared by spark plasma sintering, Journal of the American Ceramic Society 89 (6) (2006) 706–709.

[8] T. Rojac, M. Kosec, B. Malic, J. Holc, Mechanochemical synthesis of $NaNbO_3$, $KNbO_3$ and $K_{0.5}Na_{0.5}NbO_3$, Science of Sintering 37 (2005) 61–67.

[9] A. Castro, B. Jimenez, T. Hungria, A. Moure, L. Pardo, Sodium niobate ceramics prepared by mechanical activation assisted methods, Journal of the European Ceramic Society 24 (2004) 941–945.

[10] M.S. Yoon, N.H. Khansur, W.J. Lee, Y.G. Lee, S.C. Ur, Effects of $AgSbO_3$ on the piezoelectric/dielectric properties and phase transition of Li_2O doped NKN lead-free piezoelectric ceramics, Advanced Materials Research 287-290 (2011) 801–804.

[11] J.S. Kim, C.W. Ahn, S.Y. Lee, A. Ullah, I.W. Kim, Effects of $LiNbO_3$ substitution on lead-free $(K_{0.5}Na_{0.5})NbO_3$ ceramics: enhanced ferroelectric and electrical properties, Current Applied Physics 11 (2011) 149–153.

[12] Y. Wang, J. Wu, D. Xiao, B. Zhang, W. Wu, W. Shi, J. Zhu, Electrical properties and temperature stability of a new kind of lead-free piezoelectric ceramics, Journal of Physics D: Applied Physics 41 (2008) 245401.

[13] Y.Y. Wang, J.G. Wu, D.Q. Xiao, J.G. Zhu, P. Yu, L. Wu, X. Li, Piezoelectric properties of (Li, Ag) modified $(Na_{0.50}K_{0.50})NbO_3$ lead-free ceramics with high Curie temperature 459 (2008) 414–417Journal of Alloys and Compounds 459 (2008) 414–417.

[14] S. Zhang, R. Xia, T.R. Shrout, G. Zang, J. Wang, Piezoelectric properties in perovskite $0.948(K_{0.5}Na_{0.5})NbO_3$–$0.052LiSbO_3$ lead-free ceramics, Journal of Applied Physics 100 (2006) 104108.

[15] Y. Zhen, J.F Li, Normal sintering of (K,Na)NbO_3-based ceramics: influence of sintering temperature on densification, microstructure, and electrical properties, Journal of the American Ceramic Society 89 (12) (2006) 3669–3675.

[16] IRE Standards on Piezoelectric Crystals, Measurements of piezoelectric ceramics, in: Proceedings of the Institute of Radio Engineers, 49, 7, 1961, pp. 1161–1169.

[17] K. Uchino, E. Sadanaga, T. Hirose, Dependence of the crystal structure on particle size in bariumtitanate, Journal of the American Ceramic Society 72 (8) (1989) 1555–1558.

[18] B.D. Begg, E.R. Vance, J. Nowotny, Effect of particle size on the room-temperature crystal structure of barium titanate, Journal of the American Ceramic Society 77 (12) (1994) 3186–3192.

[19] Z. Yang, Y. Chang, B. Liu, L. Wei, Effects of composition on phase structure, microstructure and electrical properties of $(K_{0.5}Na_{0.5})NbO_3$–$LiSbO_3$ ceramics, Materials Science and Engineering A 432 (292) (2006) 292–298.

[20] Z.Y. Shen, Y. Zhen, K. Wang, J.F. Li, Influence of sintering temperature on grain growth and phase structure of compositionally optimized high-performance Li/Ta-modified (Na,K)NbO_3 Ceramics, Journal of the American Ceramic Society 92 (8) (2009) 1748–1752.